# 6

# Switching Mode Amplifiers for RF Applications

This chapter considers the possibilities offered to the RF PA designer by switching mode circuits. Circuits of this kind have been used for many years in dc-to-dc converter applications and appear to offer some possibilities for higher frequency use. The central issue usually is whether a typical RF power transistor at a specified frequency can ever be realistically modeled as a switching element. The straight answer to that question generally is a resounding negative, so the RF designer most frequently moves on and dismisses switching modes as being unrealizable for higher frequency applications. In fact, although the problem of "slow" switching speed can never be fully resolved at higher RF frequencies, it appears that it sometimes can be judiciously outmaneuvered and that useful RF applications do exist.

One situation in which switching-type circuits can be given more serious consideration is when a very high frequency technology is being used at a low relative frequency; a GaAs MESFET or HBT below 2 GHz would be an example. Such a device may provide sufficiently fast switching if the device is heavily overdriven. Another interesting and considerably more viable possibility is offered by the class E mode. It is shown later in this chapter how the combined controlling effects of input (gate/base) and output (drain/collector) voltage can be convoluted in a class E circuit to make an RF transistor appear to behave like a fast switch, even though it may be some way down its gain/frequency characteristic.

This chapter starts by considering a simple switching device with a broadband resistive load and then considers the effect of tuning the load. Such an amplifier, even with an ideal switching element, has surprisingly little to offer

the RF designer compared with the class B and class F modes considered in the previous chapters, but it serves as a useful introduction to the subject. The class D amplifier is next considered. In its ideal switching mode form, a "perfect" RF amplifier is created, with a half-wave rectified sinewave of current and a square-wave of voltage. This produces maximum possible fundamental RF power at 100% efficiency, but it is difficult to realize at higher RF frequencies.

The rest of the chapter considers the class E mode in some detail. The class E mode appears to have practical applications up to lower microwave frequencies and would seem to vindicate the claims made for it by its inventors over the last two decades. A specific class E design example, with measured test data, concludes the chapter.

Switching mode power amplifiers, without qualification, are highly non-linear devices. That reality leads to further rejection by the wireless communications industry, on the basis that variable envelope signals cannot be passed without hopeless levels of distortion. It should be borne in mind, however, that the same rejection could be applied equally to a class C amplifier, but such amplifiers were at one time commonly used in AM and SSB broadcasting. To overcome the distortion problem, techniques such as envelope restoration and outphasing were developed and are described in Chapter 8. Such techniques could be applied equally well to a modern class E design.

## 6.1   A Simple Switching Amplifier

Figure 6.1 is a schematic diagram of a simple switching mode amplifier. The key element is the switch, which in this analysis will be considered as ideal. By "ideal," we mean that the switch is either completely on (short circuit) or completely off (open circuit) and can switch between the two states instantaneously. Another key aspect of the idealization is that the timing of switch opening and closure is controlled by the input signal; the "conduction angle" is assumed to be discretionary in the analysis. In practice, such control of the switch conduction angle will be achieved by varying the drive level and bias point at the input of a transistor. This usually will mean that the device will be heavily overdriven in comparison to normal linear operation, and it is almost inevitable that the overall gain will be many decibels lower than a conventional linear amplifier. In any event, it will not be possible to estimate the power gain of such a circuit without more detailed knowledge of the specific device and the drive arrangements. Useful expressions, however, can be derived for the output power and efficiency.

Figure 6.1 shows an output circuit that has some familiar features: a dc-blocked RF load resistor and a choked dc supply. The current and voltage wave-
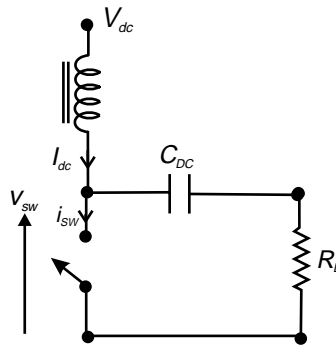
**Figure 6.1** Basic RF switching amplifier.

forms are trivial in the symmetrical case, in which the switching duty cycle is 50%. Figure 6.2 shows a more general case with a conduction angle, $2\alpha$, corresponding to the switch closure period. The maximum current in the switch is now controlled entirely by the supply voltage and the RF load resistor, and the voltage toggles between zero and $V_{pk}$, where $V_{pk}$ will be a function of the conduction angle $\alpha$ and the supply voltage $V_{dc}$. Before analyzing the waveforms in more detail, it is clear that this circuit converts dc energy to RF energy at 100% efficiency. At no point in the RF cycle is there a nonzero voltage and current simultaneously, so no energy is wasted as heat in the switch. This sometimes is interpreted erroneously as a perfect and final solution to RF power generation.
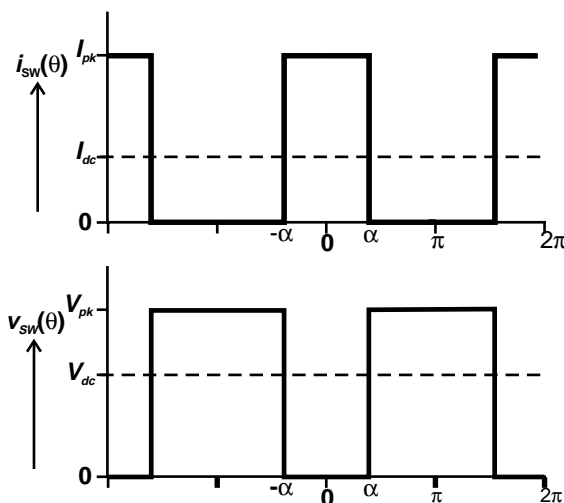


**Figure 6.2** Basic RF switch waveforms.

In fact, this particular switching mode amplifier has some undesirable characteristics, in that substantial energy is generated at harmonic frequencies, and the maximum fundamental efficiency is only just over 80%.

It is assumed that the dc supply voltage remains constant as the conduction angle $\alpha$ is varied; this will result in an asymmetrical voltage waveform whose peak value will be proportionately greater or less than twice the supply voltage as $\alpha$ is varied above or below $\pi/2$. This circuit now can be analyzed for power and efficiency as a function of the conduction angle. With a simple broadband resistive load, the relationship between the peak voltage $V_{pk}$ and the dc supply voltage $V_{dc}$ is given by the mean value integral,

$$V_{dc} = \frac{1}{2\pi} \int_{-\pi}^{\pi} v_{sw}(\theta)d\theta$$

$$= \frac{1}{\pi} \int_{\alpha}^{\pi} V_{pk} d\theta \tag{6.1}$$

$$\frac{V_{dc}}{V_{pk}} = \frac{(\pi - \alpha)}{\pi}$$

The voltage waveform can be considered to be an alternating voltage with zero mean value if it is offset by $V_{dc}$. So the peak-to-peak current swing will be $V_{pk}/R_L$ and

$$I_{pk} = V_{pk} / R_L \tag{6.2}$$

It should be noted here that an ideal switch differs from a real device in the important respect that the peak current is entirely a function of the dc supply and the load resistor $R_L$; the resistor can be arbitrarily reduced in value to give any desired amount of RF power. This analysis, therefore, will consider primarily the power and efficiency for a given value of $I_{pk}$, which can then be used as a rational equivalent for comparison to a transistor having a maximum or saturated current, $I_{max}$, equal to $I_{pk}$.

Mean value considerations for the current waveform give, by simple inspection

$$I_{dc} = \frac{\alpha}{\pi} I_{pk} \tag{6.3}$$

The fundamental even Fourier coefficient of current, $I_1$, is given by

$$I_1 = \frac{1}{\pi} \int_{-\pi}^{\pi} i_{sw}(\theta)\cos(\theta)d\theta \tag{6.4}$$

where

$$i_{sw}(\theta) = I_{pk}, \quad -\alpha < \theta < \alpha$$
$$= 0, \quad -\pi < \theta < \alpha, \; \alpha < \theta < \pi$$
$$= \frac{2}{\pi} \int_0^\alpha I_{pk} \cos(\theta) d\theta \qquad (6.5)$$

$$\frac{I_1}{I_{pk}} = \frac{2\sin(\alpha)}{\pi}$$

Similarly, the fundamental Fourier coefficient for the voltage waveform is

$$\frac{V_1}{V_{pk}} = -\frac{2\sin(\alpha)}{\pi} \qquad (6.6)$$

Combining (6.1) through (6.6), the RF power, $P_{rf}$, can be expressed in terms of the dc supply terms, $V_{dc}$ and $I_{dc}$:

$$\frac{V_1}{V_{dc}} = -\frac{2\sin\alpha}{\pi - \alpha}$$

$$\frac{I_1}{I_{dc}} = \frac{2\sin\alpha}{\alpha} \qquad (6.7)$$

$$P_{rf} = V_{dc}I_{dc}\frac{2\sin^2\alpha}{\alpha(\pi - \alpha)}$$

So that the output efficiency, $\eta$, is given by

$$\eta = \frac{2\sin^2\alpha}{\alpha(\pi - \alpha)} \qquad (6.8)$$

In the symmetrical squarewave case, the efficiency is $(8/\pi^2)$, about 81%. Figure 6.3 shows a plot of efficiency versus conduction angle. The RF efficiency peaks at the symmetrical case of $\alpha = \pi/2$, corresponding to the generation of a maximum proportion of RF energy at the fundamental. Figure 6.3 also shows the RF output power at the fundamental and at the second and third harmonics. The power curves are calibrated relative to the RF power from a class A linear amplifier having the same peak RF current (i.e., $I_{max} = I_{pk}$). Substituting for $I_{dc}$ in (6.3), the expression for fundamental RF output power (6.7) becomes:

$$P_1 = V_{dc}I_{pk}\frac{2\sin^2\alpha}{\pi(\pi - \alpha)} \qquad (6.9)$$
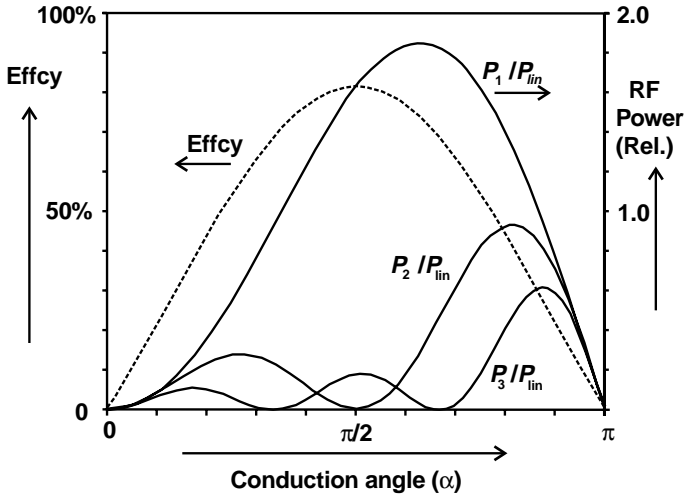
**Figure 6.3** RF output power and efficiency of basic RF switch. Fundamental and harmonic power are expressed relative to $P_{lin}$, the class A RF power having the same peak RF current at the same dc supply voltage.

and defining the linear power, $P_{lin}$ as

$$P_{lin} = \frac{V_{dc}I_{pk}}{4}$$

the relative power is

$$\frac{P_1}{P_{lin}} = \frac{8\sin^2\alpha}{\pi(\pi - \alpha)} \tag{6.10}$$

This function is also plotted in Figure 6.3. The striking feature of the fundamental power curve is the peak that occurs at a conduction angle of about 113 degrees ($\alpha = 0.63\pi$). That peak represents an RF power that is 2.7 dB higher than a class A amplifier having the same peak RF current and dc supply voltage (note that the dc supply current will be higher in the switching case). The occurrence of the peak for rectangular switching waveforms is in some respects analogous to the peak in power shown in the class AB region on a similar plot for conventional reduced conduction amplifiers (Figure 3.4); the conduction angle for maximum power appears to be similar in both cases. The peak power shown in Figure 6.3 probably represents something of a global maximum for RF power obtainable from any kind of device under the stipulated conditions and is clearly idealized.

The efficiency curve, shown dotted in Figure 6.3, represents something of a disappointment. Despite having a device that dissipates no heat, the efficiency peaks at about 81%, corresponding to the symmetrical squarewave condition. The problem, as shown by the harmonic power plots, is that power is being wasted in harmonic generation; the next step is to eliminate this using a resonator.
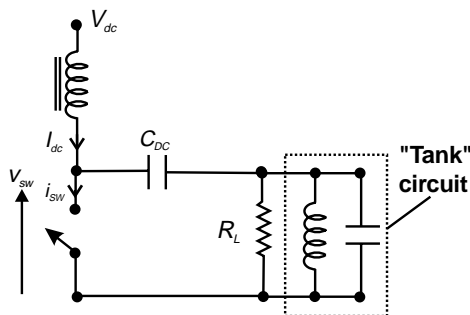
## 6.2  A Tuned Switching Amplifier

Other than the possibility for frequency multiplication, the harmonic energy indicated in Figure 6.3 is undesirable and can be most easily removed by placing a harmonic short across the load, as shown in Figure 6.4. This is more familiar territory, since the voltage waveform will now assume a sinusoidal form, as shown in Figure 6.5. This makes analysis quite straightforward. It will again be convenient to relate the current waveforms to a specific peak value, $I_{pk}$, to compare the results with that of a conventional reduced conduction mode amplifier having the same maximum peak RF current. The relationships for the current are the same as in (6.3) and (6.5):

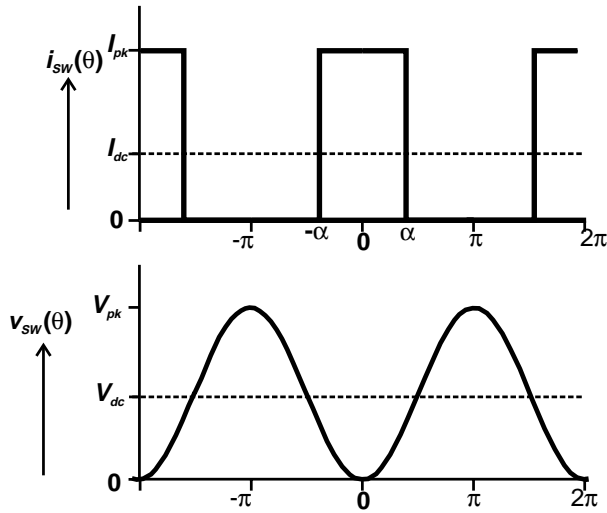$$\frac{I_1}{I_{pk}} = \frac{2\sin(\alpha)}{\pi}$$

$$\frac{I_{dc}}{I_{pk}} = \frac{\alpha}{\pi}$$

The sinusoidal voltage gives the simple relationship

$$V_1 = V_{dc}$$



**Figure 6.4**  Tuned RF switching amplifier.

**Figure 6.5** Tuned switch waveforms.

so the fundamental RF power is

$$P_1 = I_{dc}V_{dc}\frac{\sin(\alpha)}{\alpha} \tag{6.11}$$

giving this output efficiency:

$$\eta = \frac{\sin(\alpha)}{\alpha} \tag{6.12}$$

The relative power can be determined as before, by expressing $P_1$ (in 6.11), in terms of the peak current $I_{pk}$, using the relationship of (6.3):
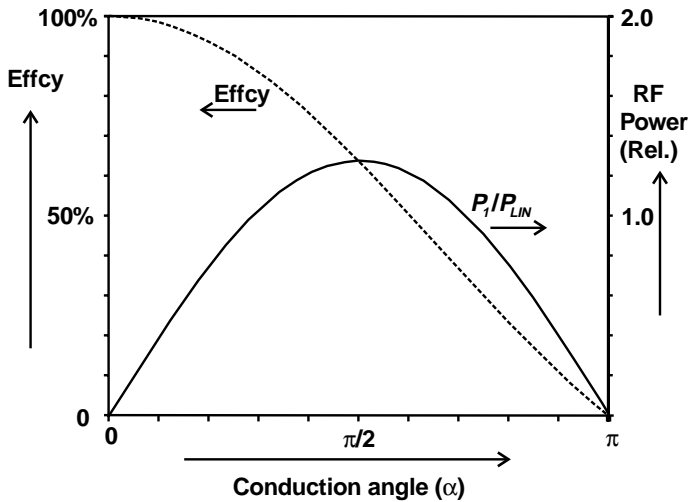
$$P_1 = I_{pk}V_{dc}\frac{\sin(\alpha)}{\pi}$$

so the ratio of fundamental RF power to $P_{lin}$ is

$$\frac{P_1}{P_{lin}} = I_{pk}V_{dc}\frac{4\sin(\alpha)}{\pi} \quad \left(P_{lin} = \frac{I_{pk}V_{dc}}{4}\right) \tag{6.13}$$

The efficiency, (6.12), and relative power, (6.13), are plotted as a function of conduction angle in Figure 6.6. As would be expected from the analysis of a class C amplifier, as the switched current pulse gets very short, the efficiency

**Figure 6.6** RF output power and efficiency of basic RF switch with harmonic short.

increases to high values but there is a corresponding reduction in relative RF power. The peak in RF power occurs at a conduction angle of $\pi / 2$, and the corresponding RF power is $(4 / \pi)$ times the linear equivalent, or about 1 dB higher. But the efficiency at that point is a rather modest 63% $(2 / \pi)$. Probably the most significant positive feature of the ideal switch performance in this circuit is the efficiency of about 87% at the point where the relative power crosses unity on the left side, although this still falls short of the class F results presented in Chapter 5.

The results of Sections 6.1 and 6.2 show that an ideal switch does not, by itself, give any significant improvements when compared with more conventional high-efficiency circuits, and alternative configurations have to be sought to make best use of a switching device. Two such configurations are now considered, the class D and class E modes.

## 6.3 Class D Switching Amplifiers

Figure 6.7 is a schematic diagram of a switching mode amplifier in which a series resonant circuit is connected across a two-way switch arrangement, whereby the LCR resonator is switched between a well-bypassed dc voltage generator and ground for alternate half cycles. It is assumed that the repetition cycle matches the resonant frequency of the LCR circuit and that the Q-factor is high.
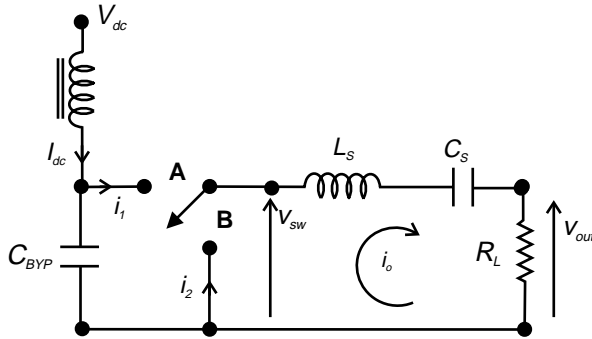
**Figure 6.7**  Switching class D amplifier.

Figure 6.8 shows the waveforms resulting from such a circuit. The key issue is that the current in the LCR branch is constrained to remain sinusoidal, with no dc offset, due to the inertia effect of the resonator and the dc blocking of the series capacitor. The result is that switch "A" conducts a positive half-sinewave, and switch "B" conducts a negative half-sinewave, which add together to form the necessary full sinewave of current in the LCR branch. Because the switch voltage waveform is a squarewave, it is clear that no power is being dissipated in the switch and that no harmonic energy is being generated; the half-sinewaves of current flowing in each switch half-cycle contain no odd harmonics. The analysis is therefore quite straightforward. The peak current, $I_{pk}$, is given by
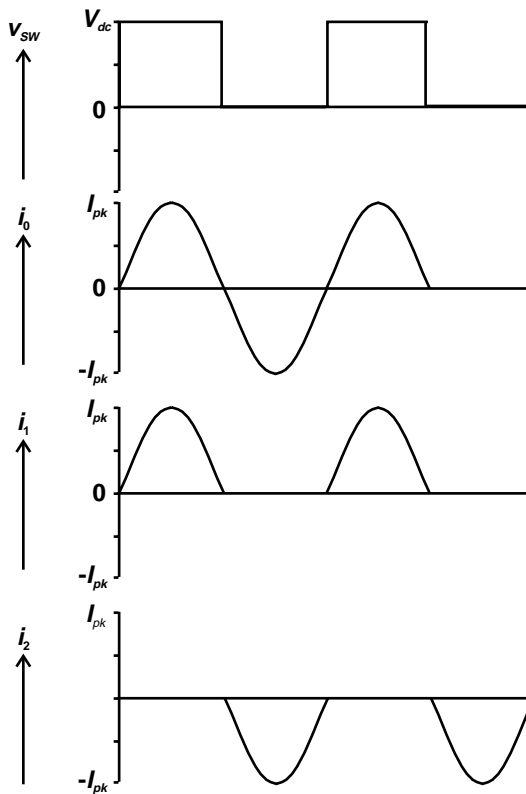
$$I_{pk} = I_{dc}\pi$$

The fundamental RF current flowing around the LCR branch, $I_1$, is simply

$$I_1 = \frac{I_{pk}}{2}$$

The fundamental component of RF voltage appearing across the LCR branch is

$$V_1 = V_{dc}\frac{2}{\pi}$$

due to the fact that the voltage appearing across the LCR branch is a squarewave of peak value $V_{dc}$. Once again, with ideal switches, the peak cur-

**Figure 6.8** Switching class D amplifier waveforms.

rent—and consequently the power—can be made arbitrarily high by suitable reduction in the value of $R_L$. The RF power can be expressed in terms of $I_{pk}$ and $V_{dc}$ from these relations:

$$P_1 = \frac{V_1 I_1}{2} = \frac{V_{dc} I_{pk}}{\pi}$$

and the dc supply power is

$$P_{dc} = V_{dc} I_{dc} = \frac{V_{dc} I_{pk}}{\pi}$$

Clearly, the efficiency is 100%. The relative power, compared to a class A device having the same $I_{pk}$ and $V_{dc}$, is

$$\frac{P_{rf}}{P_{lin}} = \frac{V_{dc}I_{pk}}{\pi} \frac{4}{V_{dc}I_{pk}} = \frac{4}{\pi}$$

about 1 dB.

This switching version of a class D amplifier has one significant difference from the RF version discussed in Chapter 5. In the switching version described here, the peak-to-peak voltage swing is equal to the dc supply voltage, and the peak-to-peak RF current is twice the peak current of each individual switching device. The switching action in some ways produces a similar overall effect to having a pair of devices in a push-pull configuration (see Chapter 10). But the overall issue is realizability. The "A" switch is a high-side (ungrounded) device that poses particularly difficult problems at higher frequencies, both in terms of parasitic reactances and driver requirements. Such amplifiers have been reported at low RF frequencies, in the 10 MHz region [1], and offer some attractive possibilities for achieving high power and high efficiency without generating excessive voltage swing. But the possibilities for low-microwave applications seem marginal at best with current technology, given the greater attractions of the class E mode.

## 6.4  Class E Switching Amplifiers

The class E mode has been vigorously touted by its inventors [2–5] for over 20 years, to a frequently ambivalent microwave community. It has also been patented, for most of that time, and the recent expiry of the patent (U.S. 3,919,656; 1975) has caused some renewed interest in the possibilities it offers [6, 7]. The next few sections are presented as a timely revisit to a technique well covered in the literature but as yet little used in the RF wireless communications industry.

The previous sections in this chapter have highlighted the difficulty of harnessing an ideal switch in a productive manner. Indeed, the results in Section 6.2 indicate that the sharp, rectangular pulses of current can be as much a hindrance in obtaining higher efficiency as they are beneficial. The class E mode in some ways represents an optimum halfway house between the analog world of conventional reduced conduction angle mode amplifiers and the digital world of ideal switches. Although it most easily is introduced as a switching type of amplifier, the waveforms are distinctly analog in appearance and can be realistically supported by a device with a slower switching characteristic that includes a linear region.

Furthermore, simulations and verification tests on actual amplifiers seem to support the view that class E truly does represent an alternative to conven-

tional reduced conduction angle operation, giving higher efficiency without the circuit complexity of more advanced class F designs. Direct comparison is troublesome, in that class F can, as was demonstrated in Chapter 5, achieve very high efficiencies but show substantially reduced power output under optimum efficiency operation. Class E has its own disadvantage in terms of peak voltage levels, and the PUF has to be traded against that limitation. Although numerous techniques have been demonstrated that can alleviate the peak voltage problem, they all involve more circuitry. But the final judgment may be that class E simply is easier to realize in practice using solid state transistors than a short conduction angle class C design.

As stated at the beginning of this chapter, a class E amplifier is unquestionably nonlinear, in the sense that variations in input power amplitude will not be reproduced at the output in any acceptable form. This also applies to a class C amplifier, and techniques have been available for several decades to remodulate the output. For reasons that are not entirely clear, these techniques have fallen into disuse somewhere along the road of transition from vacuum tubes to solid state devices. One possible reason for the change of emphasis from remodulation to linear or quasi-linear RF amplification may be that there has never been a reliable method of achieving efficiencies in the 90% region using solid state devices, such as were quite normally obtained from simple tube amplifier designs, which still can be found even in amateur radio literature. Another reason is the virtual disappearance of amplitude-only modulation systems. As will be discussed in Chapter 8, although most remodulation techniques can be adapted to preserve phase modulation, that usually incurs more system complexity.

The class E mode may just represent a possibility for achieving high-enough efficiencies from solid state devices that techniques such as envelope restoration and outphasing may become worthwhile. The analysis presented here is idealized and assumes initially that the active device can be represented as a switch. This results in some analytical expressions for the circuit design parameters. The analysis uses a similar set of starting assumptions to that published by Raab [3], but has some simplifications in mathematical formulation that lead to a more compact set of results. It should be emphasized that in keeping with much of the analysis in this book, the simplifications have been made possible by the use of very idealized device and circuit models. The works of the referenced authors allow for device and circuit parasitics and should be consulted if a class E design is being seriously contemplated.

### 6.4.1  Simplified Analysis

Figure 6.9 shows the basic elements of a class E circuit. The ideal switch is shunted by a capacitor, which is an important part of the RF network and is
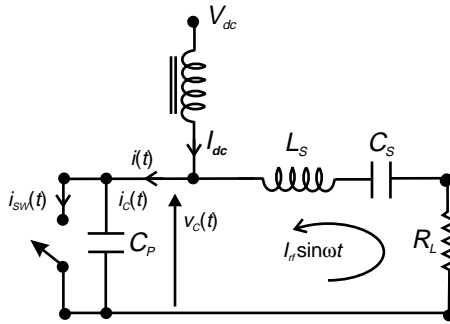
**Figure 6.9** Schematic of basic class E amplifier.

usually neither small enough to be a device parasitic nor large enough to be a harmonic short. The RF matching network consists additionally of a series resonant circuit, which contains the final RF load resistor. It is assumed in this analysis that this resistor probably will be the input impedance of an additional matching section that transforms the required value up to a 50Ω interface. As usual, the dc is supplied through a high-reactance choke whose value is such that no variations of current can be supported within the time frame of an RF cycle. Similarly, the Q-factor of the resonator is assumed to be high enough that the flywheel effect forces a pure sinewave of current to flow in the LCR branch.

As before, it is assumed that conditions on the input can be controlled such that the open and closure timing of the switch during an RF cycle can be arbitrarily predetermined and are effectively independent variables in the problem.

Looking now at the branch currents in Figure 6.9, we can see that two "irresistible" currents combine to flow into the switch-capacitor combination: the dc supply current, $I_{dc}$, and the sinusoidal flywheel current in the LCR branch, $I_{rf} \sin \omega t$.

Thus, the current flowing into the switch-capacitor combination is an offset sinewave of current,

$$i(\theta) = I_{rf} \sin(\theta) + I_{dc} \quad (\theta = \omega t)$$

where the values of $I_{rf}$ and $I_{dc}$ have yet to be determined.

Figure 6.10(a) shows the offset sinewave of current $i(\theta)$ and also shows the positions selected for switch opening and closure. The switch will be closed for the duration of the interval between the positive-moving zero crossing of $i(\theta)$, $\beta$, and an arbitrarily selected angle $\alpha$ during the positive portion of $i(\theta)$. Clearly, when the switch is closed, $i(\theta)$ will flow entirely through the switch; when the
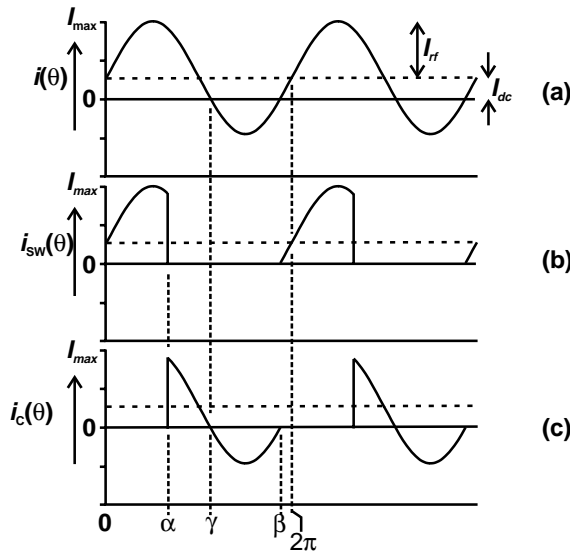
**Figure 6.10**  Class E RF current waveforms: (a) total current; (b) switch current; (c) shunt capacitor current.

switch is opened, $i(\theta)$ will flow *entirely into the capacitor*. This is the single most definitive aspect of ideal class E operation.

The current waveforms for switch and capacitor can be easily drawn and are shown in Figure 6.10(b) and (c). As already noted, the key effect is the instantaneous transfer of current from switch to capacitor at the point of switch opening, but note that when the switch closes, it does so at an instant of zero current. The current waveform in the switch bears some resemblance to a lower conduction angle, class C amplifier, with the important difference that it is highly asymmetrical with a slow rise and a very fast, ideally instantaneous, fall. The peak switch current, $I_{pk}$, is defined as

$$I_{pk} = I_{rf} + I_{dc}$$

and as before, will bear a close relationship to the $I_{max}$ of the transistor that ultimately will have to approximate the switching function.

This is a class E amplifier; all that remains is to integrate the capacitor current to obtain the RF voltage waveform and to relate the dependent variables $I_{rf}$, $I_{dc}$, $\beta$, $C_P$, $R_L$, and $L_S$ to the independent, or input, variables $V_{dc}$, $\alpha$, $\omega$, and $I_{pk}$.

The voltage waveform can be integrated initially, in terms of the yet to be determined parameters $I_{rf}$, and $I_{dc}$. The voltage across the capacitor, $v_C(\theta)$, is given by:

$$v_C(\theta) = \frac{1}{\omega C_p} \int_{(2\pi-\beta)}^{\theta} i_C(\theta)d\theta \qquad (6.14)$$

It is instructive to perform this integral numerically at first, to get some idea of the waveform characteristics. This is shown in Figure 6.11. The voltage waveform integrates up from zero, starting at the point the switch opens ($\theta = \alpha$) and the entire current $i(\theta)$ instantaneously transfers from the switch to the capacitor. A peak voltage is reached at the point where the capacitor current crosses zero ($\theta = \gamma$). Since there is no cyclic accumulation of charge in the capacitor, the voltage will reach zero again at the precise moment the switch closes again ($\theta = \beta$). Looking now at the current and voltage waveforms at the switch, we can make several important comments even before the necessary algebraic relationships between the various parameters have been derived.

- At no time in the cycle do current and voltage coexist at nonzero values. That implies 100% efficient conversion of dc to RF energy.
- The only dissipative element in the circuit is the load resistor, and this is visible to the switch only at the fundamental (switching) frequency. This implies that the only energy being dissipated is at the fundamental frequency.
- The voltage waveform is nonsinusoidal and axially asymmetric. This implies a mean dc level that will be lower than half the peak value.
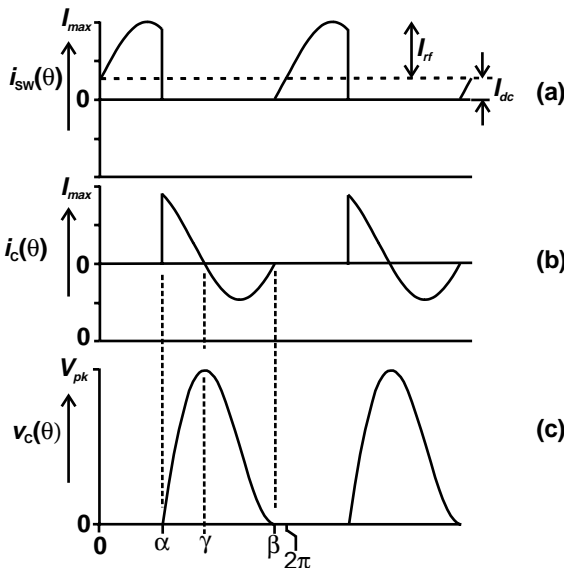


**Figure 6.11** Class E RF waveforms: (a) switch current; (b) shunt capacitor current; (c) switch/shunt capacitor voltage.

The first item in the preceding list is, of course, a direct consequence of having an ideal switch element. But taken with the second item, the important conclusion is reached that this is a 100% efficient system for converting dc to fundamental, sinusoidal RF energy, regardless of which actual value of conduction angle, α, is selected.

There is one more important observation to make on the reasoning presented thus far. From Figure 6.11, it is clear that we have created a highly nonlinear system with nonsinusoidal waveforms and an attendant galaxy of harmonic components. The normal reaction of the RF engineer to such a situation is to jump immediately into the frequency domain and start to analyze the necessary harmonic impedances. In fact, it will be seen that in this analysis the only frequency domain analysis will be to determine the fundamental components of the voltage and current waveforms; the system is effectively *solved* in the time domain. The harmonic impedances do not play any direct part in the analysis and remain as unseen elements in the problem; the network topology itself automatically provides the harmonic terminations, and we do not need to determine their values. This is not just a matter of analytical philosophy; there is a very real advantage here that we have a network that does the whole job, and not a truncated approximation to the job which we use in designing class AB or B type amplifiers. This is a subtle but very real benefit of the class E configuration.

The first step in the full analysis of the class E circuit shown in Figures 6.9 and 6.10 is to determine the essentially geometric relationships between $I_{rf}$, $I_{dc}$, α, and β. For the purposes of this analysis, the RF cycle will be considered to start at the moment of switch closure, $\theta = \beta - 2\pi$, and finish $2\pi$ radians later, with the reclosing at $\theta = \beta$.

From the geometry of an offset sinewave, the zero crossings γ and β are solutions of the equation

$$I_{dc} + I_{rf} \sin(\theta) = 0$$

or

$$\sin(\beta, \gamma) = -\frac{I_{dc}}{I_{rf}} \qquad (6.15)$$

The two solutions, β and γ, both have important significance in the subsequent analysis. β is the instant of switch closure at the end of the defined cycle, and γ is the point of zero crossing of capacitor current, which is also the instant of peak voltage. It is important to recognize, when using an inverse sine function on a computer or calculator, that β is the fourth-quadrant solution and γ is in the third quadrant:

$$\frac{3\pi}{2} < \beta < 2\pi$$

$$\pi < \gamma < \frac{3\pi}{2}$$

The relationship between $I_{rf}$ and $I_{dc}$ can be determined by recognizing that the capacitor has no mean current flow over an integrated RF cycle and that the external dc supply is equal to the mean value of the switch current:

$$I_{dc} = \frac{1}{2\pi} \int_{\beta - 2\pi}^{\alpha} \left( I_{dc} + I_{rf} \sin(\theta) \right) d\theta \qquad (6.16)$$

where the limits of integration have been set to encompass the period of switch closure.

Performing the integration, and after some rearrangement, (6.16) becomes

$$\frac{I_{dc}}{I_{rf}} = \frac{\cos \alpha - \cos \beta}{\alpha - \beta} \qquad (6.17)$$

Substituting into (6.15), a relationship between the two angles $\alpha$ and $\beta$ is obtained:

$$\sin \beta = \frac{\cos \beta - \cos \alpha}{\alpha - \beta} \qquad (6.18)$$

Clearly, this cannot be solved analytically, but from this point onward it will be assumed that for any selected value of $\alpha$, a corresponding (fourth-quadrant) value for $\beta$ easily can be computed numerically.

It later will be found convenient to measure current in terms of the peak current, $I_{pk}$. This will enable a practical design to be attempted, where $I_{pk}$ will be closely related to the $I_{max}$ of a transistor. Given that

$$I_{pk} = I_{rf} + I_{dc}$$

and defining the current offset ratio, $\varepsilon$,

$$\varepsilon = \frac{I_{dc}}{I_{rf}} = -\sin \beta$$

then

$$I_{dc} = \frac{I_{pk}}{\left(1 + \dfrac{1}{\varepsilon}\right)}$$

$$I_{rf} = \frac{I_{pk}}{(1 + \varepsilon)}$$

(6.19)

The capacitor voltage can now be determined, recalling (6.14):

$$v_c(\theta) = \frac{1}{\omega C_P} \int_{(2\pi - \beta)}^{\theta} i_C(\theta) d\theta$$

Substituting

$$i_C(\theta) = I_{dc} + I_{rf} \sin(\theta) \quad \alpha < \theta < \beta$$
$$= 0 \qquad\qquad\qquad \beta - 2\pi < \theta < \alpha$$

gives

$$v_C(\theta) = \frac{1}{\omega C_P} \int_{\alpha}^{\theta} \left[ I_{dc} + I_{rf} \sin(\theta) \right] d\theta \quad \alpha < \theta < \beta$$
$$= 0 \qquad\qquad\qquad\qquad\qquad 2\pi - \beta < \theta < \alpha$$

Performing the integration gives the relatively simple expression

$$v_C(\theta) = \frac{1}{\omega C_P} \left[ I_{dc}(\theta - \alpha) + I_{rf}(\cos \alpha - \cos \theta) \right] \quad \alpha < \theta < \beta$$
$$= 0 \qquad\qquad\qquad\qquad\qquad\qquad\qquad\qquad \beta - 2\pi < \theta < \alpha$$

(6.20)

This expression, taken along with the current normalizations in (6.19) and the conduction angle relationship in (6.18), relates the RF voltage across the switch to known quantities $I_{pk}$, $\alpha$, and the frequency $\omega / 2\pi$. The remaining unknown scaling parameter is the shunt capacitor $C_P$. This now can be determined by taking the mean value of the capacitor voltage, given in (6.20), and equating it to the known, or stipulated, dc supply voltage $V_{dc}$.

The mean voltage is given by

$$V_{dc} = \frac{1}{2\pi} \int_{\alpha}^{\beta} v_C(\theta) d\theta$$

$$= \frac{1}{2\pi\omega C_P} \int_{\alpha}^{\beta} \left[ I_{dc}(\theta - \alpha) + I_{rf}(\cos\alpha - \cos\theta) \right] d\theta$$

$$= \frac{1}{2\pi\omega C_P} \left[ \begin{array}{l} \left( I_{rf}\cos\alpha - I_{dc}\alpha \right)(\beta - \alpha) + \\ \dfrac{I_{dc}}{2}\left(\beta^2 - \alpha^2\right) - I_{rf}\left(\sin\beta - \sin\alpha\right) \end{array} \right]$$

(6.21)

For reasons that will become apparent, it pays to simplify (6.21) using the current offset relationship (6.15),

$$\frac{I_{dc}}{I_{rf}} = -\sin\beta$$

and the conduction angle relationship (6.18),

$$\sin\beta = \frac{\cos\beta - \cos\alpha}{\alpha - \beta}$$

Substituting first for $I_{dc}$ in terms of $I_{rf}$ from (6.15),

$$\frac{2\pi\omega C_P}{I_{rf}} V_{dc} = \left(\cos\alpha + \alpha\sin\beta\right)(\beta - \alpha) - \left(\sin\beta - \sin\alpha\right)$$

$$-\frac{1}{2}\sin\beta\left(\beta^2 - \alpha^2\right)$$

$$= \cos\alpha(\beta - \alpha) + \left\{ (\alpha - \beta)\sin\beta \right\}\left\{ -\alpha + \frac{1}{2}(\beta + \alpha) \right\}$$

$$-\sin\beta + \sin\alpha$$

$$= \cos\alpha(\beta - \alpha) + \frac{1}{2}(\beta - \alpha)\left\{ (\alpha - \beta)\sin\beta \right\}$$

$$-\sin\beta + \sin\alpha$$

and now substituting $(\alpha - \beta)\sin\beta = \cos\beta - \cos\alpha$, from (6.18),

$$\frac{2\pi\omega C_P}{I_{rf}} V_{dc} = \frac{1}{2}(\beta - \alpha)(\cos\beta + \cos\alpha) - \sin\beta + \sin\alpha \qquad (6.22)$$

which can be written in this form:

$$V_{dc} = \frac{1}{\omega C_P} I_{pk} v_{dc}(\alpha) \qquad (6.23)$$

where $v_{dc}(\alpha)$ is a normalized function of the selected conduction angle $\alpha$ for unity $I_{pk}$. The function $v_{dc}(\alpha)$ can be plotted out for a range of $\alpha$ values, using the other relationships in (6.18) and (6.19) that relate the currents and the conduction angles. For a selected value of $\alpha$ and a stipulated value of dc supply voltage, $\omega$, and $I_{pk}$, the value of $C_P$ can be calculated using (6.23).

At this point, all the waveforms in Figures 6.10 and 6.11 are determinate; they can be drawn precisely to scale using the input variables $\alpha$, $\omega$, $I_{pk}$, and $V_{dc}$. The problem has been solved without resorting to frequency domain analysis. Fourier analysis only at the fundamental is now required to determine the values of the circuit elements $C_P$, $L_S$, $C_S$, and $R_L$.

The "in-phase" fundamental component of the capacitor (and switch) voltage is required to determine a value for the RF load resistor, $R_L$. By "in-phase," we mean that the required voltage is in phase with the original current that was stipulated in the LCR branch, $I_{rf} \sin\theta$. The voltage component in-phase with this current is given by

$$V_{ci} = \frac{1}{\pi} \int_{\alpha}^{\beta} v_C(\theta)\sin\theta\, d\theta \qquad (6.24)$$

There also will be a quadrature component of $v_C(\theta)$, given by

$$V_{cq} = \frac{1}{\pi} \int_{\alpha}^{\beta} v_C(\theta)\cos\theta\, d\theta \qquad (6.25)$$

A nonzero value of $V_{cq}$ indicates that the phase angle of the fundamental voltage appearing across the resonant LCR branch is nonzero, which is in conflict with the original stipulation that the current in this branch has zero phase, with reference to a sinewave. That conflict can be resolved by slightly mistuning the resonator; the value of $V_{cq}$ will be used to determine a reactive offset in the resonance of the LCR elements.

The integral in (6.24) can be evaluated to give

$$V_{ci} = \frac{1}{\pi\omega C_P} \left\{ \begin{array}{l} I_{dc}\left[(\sin\beta - \sin\alpha) + \cos\beta(\alpha - \beta)\right] \\ +I_{rf}\left[\cos\alpha(\cos\alpha + \sin\alpha) - \cos\beta(\cos\alpha + \sin\beta)\right] \end{array} \right\} \quad (6.26)$$

The same process of simplification as in (6.21) will now be used. Substituting, again, for $I_{dc}$ in terms of $I_{rf}$, from (6.15),

$$\frac{\pi\omega C_P}{I_{rf}}V_{ci} = (\cos\alpha + \alpha\sin\beta)(\cos\alpha - \cos\beta) + \frac{1}{2}\left(\cos^2\beta + \cos^2\alpha\right)$$

$$- \sin\beta(\alpha\cos\alpha - \beta\cos\beta - \sin\alpha + \sin\beta)$$

Taking a factor of $(\cos\alpha - \cos\beta)$ out from the top line and substituting $(\alpha - \beta)\sin\beta = \cos\beta - \cos\alpha$ (from 6.18) gives

$$\frac{\pi\omega C_P}{I_{rf}}V_{ci} = \sin\beta\left[-(\alpha - \beta)(\cos\alpha + \alpha\sin\beta) + \frac{1}{2}(\alpha - \beta)(\cos\beta + \cos\alpha)\right]$$

$$- \sin\beta(\alpha\cos\alpha - \beta\cos\beta - \sin\alpha + \sin\beta)$$

substituting, finally, for $(\alpha - \beta)\sin\beta = \cos\beta - \cos\alpha$ in the first term of the upper bracket gives

$$\frac{\pi\omega C_P}{I_{rf}}V_{ci} = \frac{1}{2}\sin\beta\left\{(\beta - \alpha)(\cos\beta + \cos\alpha) + \sin\alpha - \sin\beta\right\} \quad (6.27)$$

Comparing (6.27) with (6.22), it is apparent that

$$\frac{2\pi\omega C_P}{I_{rf}}V_{dc} = \frac{\pi\omega C_P}{I_{rf}}\frac{1}{\sin\beta}V_{ci}$$

so that

$$\frac{V_{ci}}{V_{dc}} = 2\sin\beta \quad (6.28)$$

an intriguing triumph of algebraic manipulation, which is essentially a confirmation of the initial observation that the dc-to-RF conversion efficiency will be 100%. The RF power, $P_{rf}$, is given by

$$P_{rf} = \frac{I_{rf} V_{ci}}{2} = I_{rf} V_{dc} \sin \beta \qquad \text{(from 6.28)}$$

The dc power, $P_{dc}$, is given by

$$P_{dc} = I_{dc} V_{dc} = I_{rf} \sin \beta \, V_{dc} \qquad \text{(from 6.15)}$$

Thus, the dc-to-RF conversion efficiency, $\eta$, is

$$\eta = \frac{P_{rf}}{P_{dc}} = 1$$

The PUF can be written as

$$PUF = \frac{P_{rf}}{P_{lin}} = \frac{V_{dc} I_{pk}}{\left[ 1 + \left( \dfrac{1}{\varepsilon} \right) \right]} \frac{4}{V_{dc} I_{pk}} = \frac{-4 \sin \beta}{(1 - \sin \beta)} \qquad (6.29)$$

We note, in passing, that a PUF of unity will occur when $\sin \beta = -(1/3)$; this, by the relationship of (6.18), occurs at a conduction angle of $\alpha = 113$ degrees.

As before, it will be convenient to write (6.27) in the form

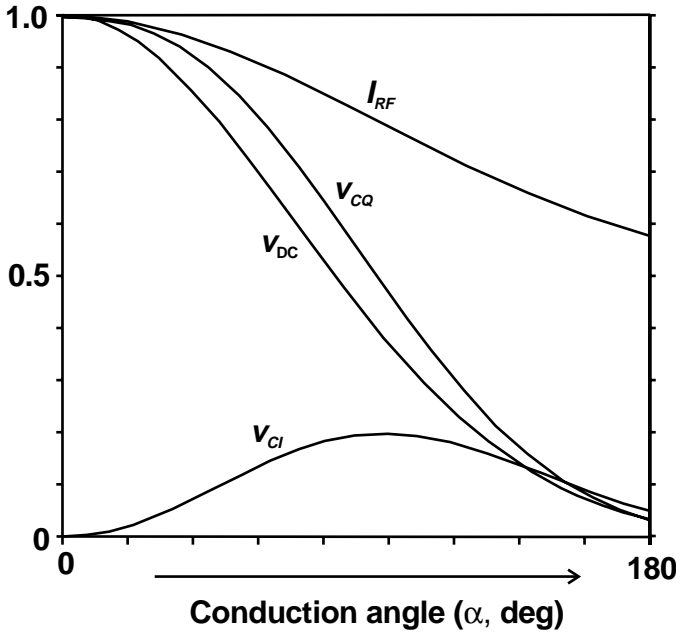$$V_{ci} = \frac{1}{\omega C_P} I_{pk} v_{ci}(\alpha) \qquad (6.30)$$

where $v_{ci}(\alpha)$ is a normalized function of conduction angle and is plotted in Figure 6.12. The value of the load resistor can now be determined, because

$$R_L = \frac{V_{ci}}{I_{rf}} \qquad (6.31)$$

and, from (6.19),

$$I_{rf} = \frac{I_{pk}}{(1 + \varepsilon)} \quad \text{or} \quad \frac{I_{pk}}{(1 - \sin \beta)} \qquad (6.32)$$

The quadrature voltage component, $V_{cq}$, is similarly obtained by performing the integral in (6.25):

**Figure 6.12** Design parameters for class E amplifier, as a function of conduction angle, $\alpha$. Currents are normalized for $I_{max} = 1$, $1/\omega C_P = 1$ (see text).

$$V_{cq} = \frac{1}{\pi\omega C_P} \left\{ I_{dc}\left[\sin\beta(\beta - \alpha) + (\cos\beta - \cos\alpha)\right] + \frac{I_{rf}}{4} \left[4\cos\alpha(\sin\beta - \sin\alpha) + 2(\alpha - \beta) - \sin 2\beta + \sin 2\alpha\right] \right\} \quad (6.33)$$

and can be written in the form

$$V_{cq} = \frac{1}{\omega C_P} I_{pk} v_{cq}(\alpha) \quad (6.34)$$

where $v_{cq}(\alpha)$ is the normalized value of $V_{cq}$ and is plotted out in Figure 6.12.

The parameter $\Delta X_S$ is now defined as

$$\Delta X_S = \frac{V_{cq}}{I_{rf}} \quad (6.35)$$

and will be an additional reactance that is added in series with the resonant LCR components to allow for the phase of the capacitor voltage.

Now that a value for $\Delta X_S$ has been determined, the actual values of $L_S$ and $C_S$ can be determined using the standard resonance relation,

$$\omega^2 L_S C_S = 1$$

The actual values of $L_S$ and $C_S$ are not uniquely defined, and essentially any resonant pair of values will work, provided the Q-factor is sufficiently high. In fact, as will be shown in an actual design example, the need to transform the load resistance to a 50Ω system termination usually will lead to a unique value for those elements.

The analysis of a class E amplifier using an ideal switch is complete. The most important outstanding issue from a design viewpoint, concerns the selection of the conduction angle, α. As shown above in relation to (6.28), the efficiency of a class E amplifier will always be 100%, regardless of the value of α. In contrast, the RF power, as measured by the PUF, is a rather strong function of α (and by direct implication, β), as shown by (6.29). Figure 6.13 shows the power, normalized as the PUF, plotted as a function of α. It would seem that higher values of α can give PUF factors well in excess of unity, but one final factor enters into the reckoning and requires a more careful compromise for the value of α. This factor is the peak voltage $V_{pk}$, also plotted in Figure 6.13 as a ratio to the dc supply $V_{dc}$. $V_{pk}$ can be calculated from (6.20), putting $\theta = \gamma$, as defined in (6.15).

Figure 6.13 shows that, although small values of α give values of $V_{pk} / V_{dc}$ only slightly higher than the conventional factor of 2, as α increases to give a PUF of unity, the peak voltage ratio increases to a factor of nearly 3 and for
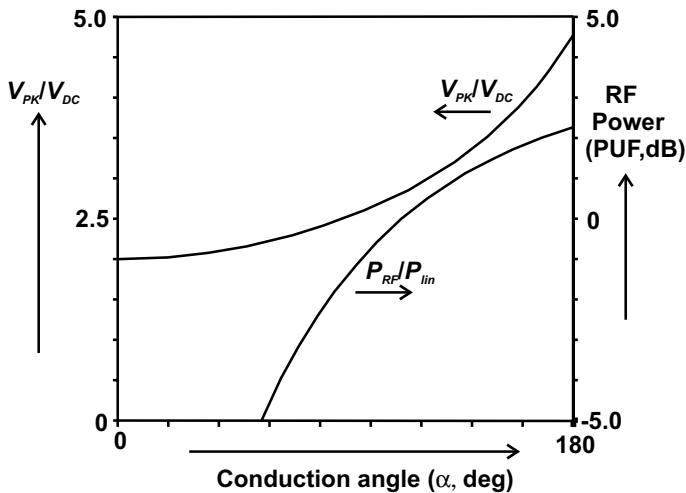


**Figure 6.13** RF output power (PUF) and peak RF voltage of class E amplifier, as a function of conduction angle, α.

PUF values significantly higher than unity the peak voltage ratio climbs still higher. This is a significant downside issue for class E operation. Obviously, in a given case, it is possible to reduce the dc supply to an appropriate level to take account of the higher peak voltage.[1] But that further reduces the available power, in comparison to a more conventional mode that has a peak voltage ratio close to 2 and would not require a lowering of the supply voltage. But there are cases when the supply voltage may be much lower, for other reasons, such as in mobile handset applications. In these cases, it is common to be using a transistor technology with much higher breakdown than is actually required based on the battery voltage available. Those applications would seem to be prime targets for class E applications.

Based on the plots shown in Figure 6.13, it would appear that the useful range of $\alpha$ for normal applications is restricted to a small range in the vicinity of 110 degrees.

### 6.4.2  Design Example

A design example will now be considered, illustrating the use and the necessary denormalization of the design chart shown in Figure 6.12. Then the big step must be taken to replace the ideal switch element with a real device. In this example, the device will be the same GaAs MESFET used in previous design examples in Chapters 4 and 5, so direct comparisons can be made. A Spice simulation will show that most of the features predicted by the analysis can be realized, despite the nonideal nature of the device. Actual measured data on a test amplifier based on the same design will then be shown.

The intention is to base the design of the same "generic" MESFET transistor used in previous chapters. As always, the first issue is to select an appropriate value for $I_{max}$, and a little foresight is needed in this case, since the device is to be forced into the role of a switch. It will be seen that this requires a lowering of the effective value of $I_{max}$ of a given device to serve as a suitable design value for $I_{pk}$ in the above equations. This involves a certain amount of trial and error using a nonlinear simulator. In the case in question, the device had a working value of about 2.5A for class A through B design purposes; for class E applications, a value of $I_{pk} = 1.0$A will be taken. This may seem a big step down in current and is indeed a foretaste of the penalties involved in making RF power transistors behave like fast switches. But it should be recalled from the results and discussions in Chapters 4 and 5, that pushing for

---

1. There is some inconsistency in the literature on how to define PUF; in these cases some authors base the power criterion on peak voltage, rather than DC.

rail-to-rail voltage swings to obtain higher efficiencies inevitably results in much reduced peak RF currents, even for overdriven reduced conduction angle modes. There are benefits that will in some cases outweigh this singular drawback.

Using the chart in Figure 6.12, and selecting a value for $\alpha$, as discussed of 110 degrees, four normalized parameters can be determined:

$$v_{dc} = 0.30; \; v_{ci} = 0.19; \; v_{cq} = 0.385; \; I_{rf} = 0.76$$

Along with the given parameters of frequency, $\omega / 2\pi$, and dc supply voltage, $V_{dc}$, the circuit element values can be obtained as follows:

1.  Shunt capacitor $C_P$: referring to (6.23), the value of $C_P$ is given by

$$\frac{V_{dc}}{v_{dc}} = \frac{1}{\omega C_P}$$

    giving $X_C = 4.8 / 0.3 = 16\Omega$, so at 850 MHz, $C_P = 11.7$ pF

2.  Load resistor $R_L$: referring to (6.31), the value of $R_L$ is given by

$$\frac{V_{ci}}{I_{rf}} = \frac{0.19}{0.76} \frac{4.8}{0.3} = 4.0\Omega$$

    Note that the normalized value of $v_{ci}$, like the value of $v_{dc}$ in step 1 needs to be scaled by the same factor of $1 / (\omega C_P)$.

3.  Reactive mistuning element $\Delta L$: referring to (6.35), the value of $\Delta X$ is given by

$$\frac{V_{cq}}{I_{rf}} = \frac{0.385}{0.76} \frac{4.8}{0.3} = 8.1\Omega$$

    so at 850 MHz, that is an inductance of 1.5 nH.

4.  Series resonant circuit elements: at this stage, these elements are not uniquely determined, and it is necessary to select only a reasonable value of Q, say 10, which gives an inductance of

$$\omega X_S = 40, \quad \text{or} \quad L_S = 7.5 \text{ nH}$$

    Thus, the series resonant capacitor has a value of $C_S = 4.7$ pF.

At this point, it normally would be necessary to design an additional matching network to transform the 4Ω load resistor up to 50Ω. This will be illustrated shortly, but the circuit can be simulated in its present form.

The Spice simulation waveforms for transistor output current and voltage are shown in Figure 6.14, along with the relevant Fourier components for calculating power and efficiency (see Figure 6.15 for schematic and Appendix A for a file listing). Simple visual inspection of the waveforms shows a remarkable similarity to the idealized plots in Figures 6.10 and 6.11; the current has the characteristic asymmetrical appearance, and the voltage has the predicted triangular form. The RF power is 1.06W, or 30.25 dBm; that is as much as 2 dB lower than some of the results using the same device model in Chapters 4 and 5. But the efficiency is a spectacular 89%, which is achieved using the direct computed element values, with no further adjustment. To achieve the necessary switching action from the device, it has been biased below its pinchoff point ($V_b = -2.75$, for $V_t = -2.5$) but the drive has been maintained at the same maximum level used in the reduced conduction angle high efficiency amplifier simulations in Chapter 4 (e.g., Figure 4.15 et seq.).
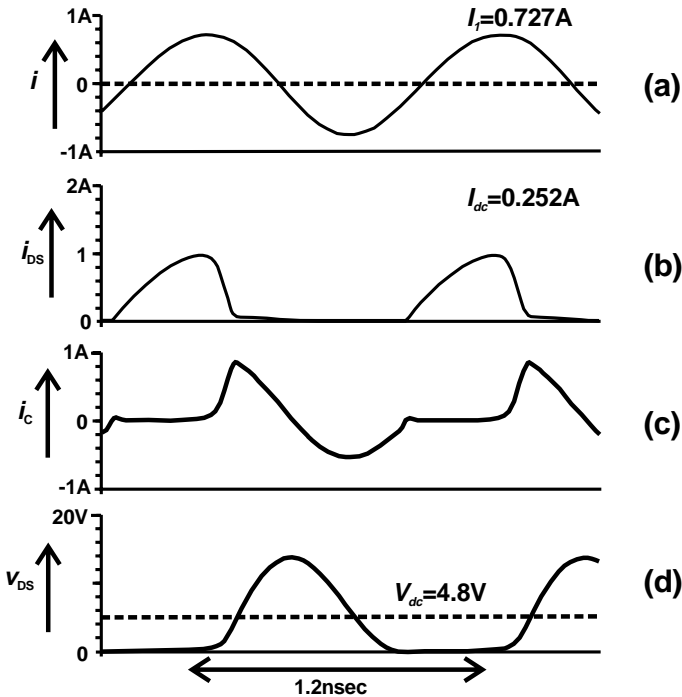


**Figure 6.14**  Spice simulation of class E design shown in Fig. 6.14: (a) 4Ω load resistor current; (b) transistor drain current; (c) shunt output capacitor current, (d)transistor output voltage.
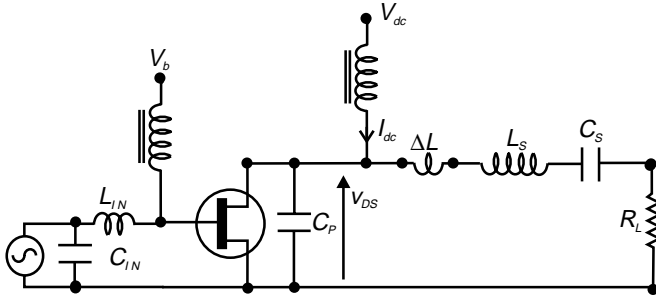
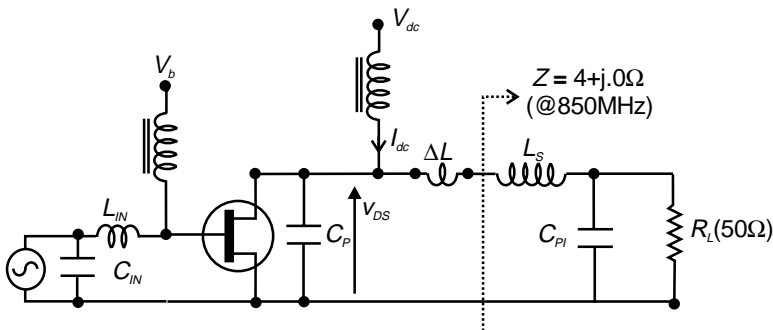**Figure 6.15** Class E amplifier design. Frequency 850 MHz, $\alpha = 110°$, $I_{max} = 1$, Vdc = 4.8V.

The results are promising, so the final step in the design process has to be taken, which is to transform the load resistor up to 50Ω. That can be done using the same matching process described in Chapter 4. The series R-C part of the resonator can be transformed to a parallel R-C, in which the shunt resistor is specified to be 50Ω.

By using (4.1) and (4.2) and referring to Figure 6.16, the transformation ratio *n* will be 50 / 4 = 12.5. So the value of shunt capacitance is given by

$$X_{PI} = \frac{50}{\sqrt{n-1}} = 14.7\Omega$$

so $C_{PI} = 12.7$ pF at 850 MHz.

From (4.2), the series resonating inductance, $X_S$ will now have a different value given by



**Figure 6.16** Class E amplifier design, showing modification of output network to incorporate a 4Ω to 50Ω impedance transformation.

$$X_S = 4.\sqrt{n-1} = 13.6\Omega$$

so $L_S$ = 2.6 nH at 850 MHz.

The mistuning element, $\Delta L$, will be unaffected by this transformation, so the final circuit is shown in Figure 6.16. A Spice simulation (not illustrated) shows almost identical performance to the original plots in Figure 6.14, despite a significant lowering in the Q-factor of the resonance, which is incurred as a result of incorporating the impedance transformation.

A closer scrutiny of the voltage and current waveforms, shown in Figure 6.17, gives some qualitative indication of how the transistor gives a similar set of waveforms compared to that of an ideal switch. The key is a small ramp of voltage that delays the full turn-on of the device, despite being in the conduction half-cycle of gate voltage. This ramp gives the current pulse, which otherwise would be a half-wave rectified sinewave of much greater peak amplitude (shown dotted), an asymmetrical appearance as required by the class E equations. Thus, the action of a switch can be mimicked but with a substantial penalty in peak current swing. So the main action of a class E amplifier takes place within—and is indeed critically dependent on—the knee region of the I-V characteristic; a unique feature that was emphasized by Sokal [2].

The original estimate for $I_{pk}$ was based on some knowledge of the above considerations, and the simulation does show a peak current around that
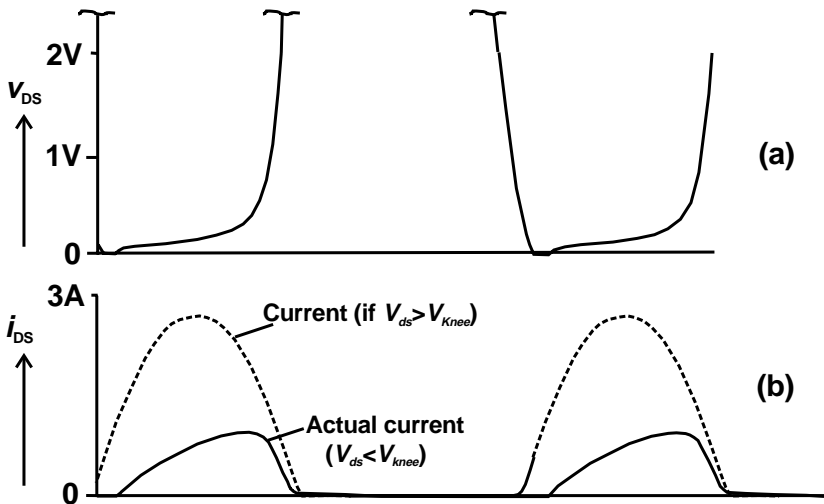


**Figure 6.17** Class E quasi-switching action: (a) magnified drain-source voltage showing ramp-up in knee region; (b) drain current, showing modulating effect of drain-source voltage; dotted trace is current under same bias and drive conditions but with RF voltage maintained above knee level.

value. Some attempt to obtain a higher peak current by scaling the design parameters can be attempted, but true class E operation will be compromised at higher $I_{pk}$ values due to the slower "quasi-switching" speed. In fact, it is instructive simply to vary the value of $C_P$. around its design value. The results, shown in Figure 6.18, show a broad tradeoff between power and efficiency with a promising plateau of efficiency values in excess of 90%. It appears that a slightly lower value of $C_P$ in this design would yield almost 1 dB higher power for a minimal loss in efficiency of one or two percentage points. As always, however, with a class E design, the peak voltage needs to be watched; this design is based on a low supply voltage. As the value of $C_P$ departs more substantially away from the design value, the amplifier behavior departs from true class E operation but shows a possibly more favorable and certainly comparable power-efficiency tradeoff than the class F results for the same transistor (indicated in Figure 5.16).

Figure 6.18 demonstrates the importance of the shunt capacitor value. Once again, as in Chapter 4, we find that this element has a strong effect on the PA characteristics, yet it is an element that is rarely adjusted and often inaccessible in practice. Its value in most of the sweep in Figure 6.18 is much higher than the transistor output capacitance, so it is necessary to enhance the transistor output capacitance, preferably with an on-chip element, or as a minimum with a low-inductance chip placed right next to the transistor die. This is an unpopular technique for RF designers, not to mention device technologists, who strive to minimize transistor parasitics to increase their high-frequency performance.
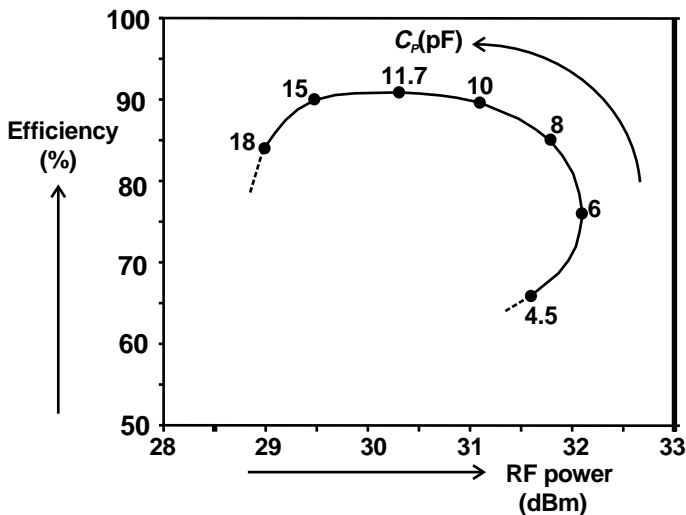


**Figure 6.18** Effects of varying the shunt output capacitor, $C_P$.

As with the harmonic stubs considered in Chapter 4, the placement issue can become a serious problem when large packaged transistors are used and is probably a leading cause of failure in class E designs at higher frequencies. It also should be fairly stated that a typical load-pull tuner is unlikely to be able to simulate the combined effects of a prescribed shunt capacitor and tunable load resistor simultaneously. The shunt capacitor needs to be supplied; then the tuner can do a much more productive job of varying the load impedance.

Figure 6.19 shows some measured data from an amplifier constructed using the design parameters in Figure 6.18, with $C_P$ about 8 pF. Power and efficiency are both plotted on linear scales to illustrate the possibility for using the
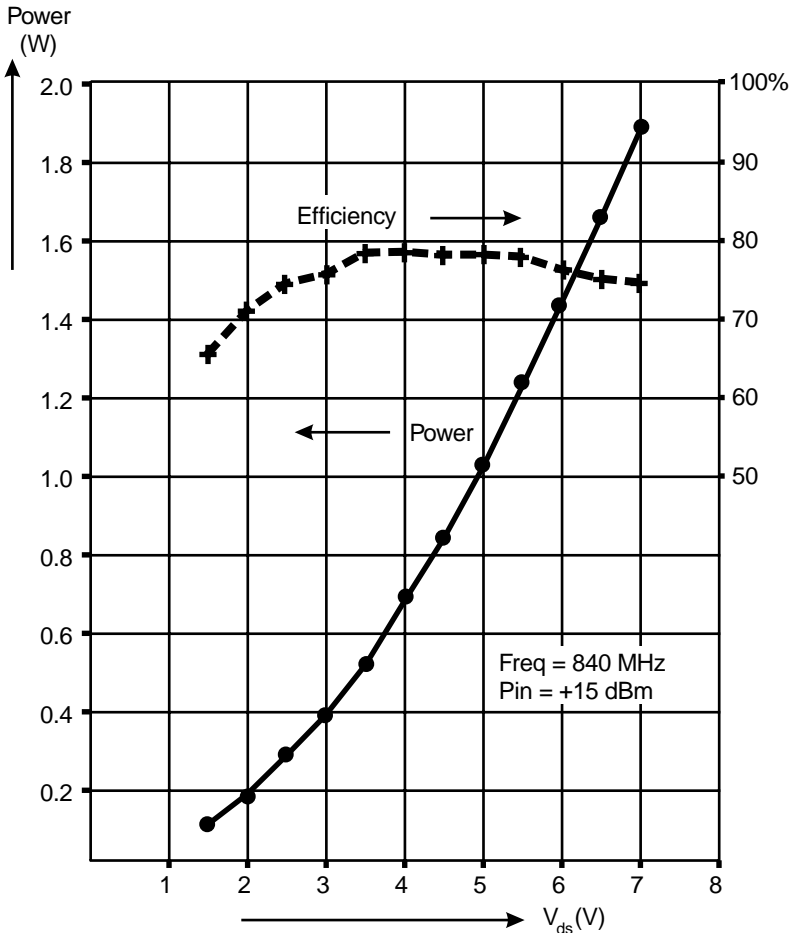


**Figure 6.19**  Measured performance of class E amplifier.

supply voltage to generate or restore amplitude modulation. The efficiency can be seen to hold up very well over a very wide range of supply voltage.

## 6.5  Summary

This chapter has shown that class E is a viable and potentially useful mode of RF power amplification. Simple design equations were shown to yield useful designs that can be verified in practice. Theoretical efficiencies of around 90% can be achieved, albeit with an RF output power as much as 2 dB lower than that obtainable from the same device in a conventional class AB configuration. Class E amplifiers are highly nonlinear, but they offer possibilities for envelope restoration techniques.

On the downside, peak voltages can be as high as three times the dc supply. Although some techniques have been proposed to overcome that problem, it is not clear whether they are fully applicable at higher frequencies into the gigahertz region. A device with a given breakdown voltage usually can be operated in class AB at a supply voltage half that level. If a class E design requires the voltage to be dropped to one-third the breakdown level, it is only fair to take account of that in the PUF calculation. There is also the issue of power gain. If a typical class E amplifier is running at a 3–5 dB lower power gain than a comparable linear amplifier due to the overdrive requirements on the input, the upper frequency limit will be lower for a given technology. Generally speaking, 12–13 dB linear gain would be required from a given device to stand a chance of useful class E operation; however, the same can be said of conventional high-efficiency modes with shorter conduction angles.

The really critical advantage of the class E amplifier is efficiency. With the possibility of reaching into the 90-percentile range, the advantages of low heat generation offer some novel concepts in packaging, modulation, and power combining. As a minimum, it is a technique that deserves closer scrutiny than it has received hitherto from the RF communications industry.

## References

1.  El-Hamamsy, S., "Design of High-Efficiency RF Class D Power Amplifier," *IEEE Trans. Power Elect.*, Vol. 9, No. 3, May 1994.

2.  Sokal, N. O., and A. D. Sokal, "Class E—A New Class of High Efficiency Tuned Single-Ended Power Amplifiers," *IEEE J. Solid State Circuits*, SC-10, No. 3, pp. 168–176, June 1975.

3.    Raab, F. H., "Idealized Operation of the Class E Tuned Power Amplifier," *IEEE Trans. Circuits and Systems*, CAS-24, No. 12, Dec. 1977.

4.    U.S. Patent 3,919,656, "High-Efficiency Tuned Switching Power Amplifier."

5.    Sokal, N. O., "RF Power Amplifiers, Classes A Through S, et seq.," *Proc. Wireless and Microwave Technology '97*, Chanatilly, VA.

6.    Imbornone, J., et. al., "A Novel Technique for the Design of High Efficiency Power Amplifiers," *Proc. European Microw. Conf.*, Cannes, 1994.

7.    Mader, T., et. al., "High Efficiency Amplifiers for Portable Handsets," *Proc. IEEE Conf. on Personal, Indoor, and Mobile Comms.*, Toronto, 1995, pp. 1242–1245.